Symmetry-Guided Design and Fluorous Synthesis of a Stable and Rapidly Excreted Imaging Tracer for (19)F MRI

ARTICLE *in* ANGEWANDTE CHEMIE INTERNATIONAL EDITION · FEBRUARY 2009

Impact Factor: 11.26 · DOI: 10.1002/anie.200901005 · Source: PubMed

4 AUTHORS, INCLUDING:

Zhong-Xing Jiang
Wuhan University
41 PUBLICATIONS **664** CITATIONS
SEE PROFILE

Eun-Kee Jeong
University of Utah
121 PUBLICATIONS **2,548** CITATIONS
SEE PROFILE

Published in final edited form as:
Angew Chem Int Ed Engl. 2009 ; 48(26): 4755–4758. doi:10.1002/anie.200901005.

Symmetry-guided Design and Fluorous Synthesis of A Stable and Rapidly Excreted Imaging Tracer for ^{19}F MRI**

Zhong-Xing Jiang,
Fischell Department of Bioengineering, University of Maryland, College Park (USA)

Xin Liu,
Department of Physics, University of Utah, Salt Lake City, (USA)

Eun-Kee Jeong [Prof.], and
Department of Radiology, University of Utah, Salt Lake City (USA)

Yihua Bruce Yu [Prof.]*
Department of Pharmaceutical Sciences, University of Maryland, Baltimore (USA), Fischell Department of Bioengineering, University of Maryland, College Park (USA)

Keywords

dendrimers; ^{19}F MRI; imaging agent; modular symmetry; perfluoro-*tert*-butanol

^{1}H and ^{19}F are the most sensitive nuclei for nuclear magnetic resonance imaging (MRI), with the ^{1}H signal suited for collecting information of the body[1,2] and the ^{19}F signal suited for collecting information of drugs in the body.[3,4] Although ^{19}F MRI[5] is only four years younger than ^{1}H MRI,[6] it is not in clinical use. The progress of ^{19}F MRI has been stalled by lack of suitable imaging agents. Current ^{19}F imaging agents are perfluorocarbon (PFC) emulsions[7–13] and suffer severe shortcomings, including heterogeneity, instability, split ^{19}F signal, complex formulation procedure and, most importantly, excessive organ retention for months or longer.[8,14] We developed a bi-spherical fluorocarbon molecule, denoted as ^{19}FIT to stand for ^{19}F imaging tracer, which overcame all the major deficiencies of PFC-based imaging agents. ^{19}FIT, designed using the principle of modular spherical symmetry, is water-soluble and emits a single ^{19}F signal from 27 fluorine atoms. The *in vivo* residence half-life of ^{19}FIT measured in mice is about 0.5 day, and no evidence of organ retention or *in vivo* degradation was found. Our result shows that modular symmetry is a useful strategy for designing molecules with multi-functionalities. With suitable imaging agents like ^{19}FIT, ^{19}F MRI has the potential to play an important role in drug therapy, analogous to the role played by ^{1}H MRI in disease diagnosis.

MRI has made significant contribution to medical diagnosis.[15] The value of MRI comes from its ability to collect *in vivo* information non-invasively without ionizing radiation.[16] ^{1}H and ^{19}F are respectively the most and second most sensitive stable nuclei for MRI. Due to the ubiquitous presence of the ^{1}H signal and the complete absence of the ^{19}F signal in the human body, ^{1}H and ^{19}F MRI complement each other in their information content. ^{1}H MRI is suited for collecting information of the body (anatomy, physiology and biochemistry) and

**This work was supported by NIH grants (EY015181 & EB004416), the Maryland Nano-Biotechnology Fund and the University of Utah seed incentive grant. We thank Dr. Yong-En Sun for assisting with animal handling.

*Fax: (+1) 410-706-5017 byu@rx.umaryland.edu.

Supporting information for this article is available on the WWW under http://www.angewandte.org or from the author.

therefore is a valuable tool for disease diagnosis. ^{19}F MRI, on the other hand, is a tracer-type technology and is suited for collecting information of drugs in the body (where, how much and in what form), and therefore has the potential to become a valuable tool for image-guided drug therapy.

Direct monitoring of drugs by ^{19}F MRI requires the drug to be labeled by appropriate ^{19}F imaging agents. For more than three decades, PFC emulsions have been used as ^{19}F imaging agents.[5,7–13] However, PFC emulsions suffer severe drawbacks as imaging agents. First and foremost, PFCs are very lipophilic and accumulate excessively in internal organs (liver, spleen, lung) for months or longer.[8,14] Second, emulsion droplets are inherently heterogeneous, unstable, and are likely to disintegrate inside the body. In fact, the *in vivo* integrity of PFC droplets is difficult, if not impossible, to verify. Third, linear PFCs emit multiple ^{19}F signals due to lack of symmetry. Signal splitting lowers signal intensity and can cause image artifacts. Macrocyclic PFCs (e.g., perfluoro-15-crown-5 ether, or PF15C5) will also emit multiple ^{19}F signals if convalently modified because their cyclic symmetry will then be broken. Finally, the formulation of PFC emulsions is quite complex, requiring multiple surfactants and microfluidic devices.[11–13] Complex formulation brings a range of difficulties for industrial production and regulatory approval. Indeed, there is currently only one injectable emulsion, Diprivan®, in the US market.[17]

All the aforementioned shortcomings of PFC-based imaging agents can be avoided if a hydrophilic stable molecule that emits a single ^{19}F signal from multiple fluorine atoms can be developed. To achieve this goal, we employed a molecular design principle called modular spherical symmetry. A molecule with modular spherical symmetry comprises independent spherical cones joined by covalent bonds in the cone part. The fluorocarbon molecule, ^{19}FIT, contains an F-spherical cone and an H-spherical cone (Figure 1). Spherical symmetry in the F-spherical cone ensures a single ^{19}F signal from multiple fluorine atoms. Spherical symmetry in the H-spherical cone allows efficient incorporation of multiple hydrophilic groups. The advantage of spherical cones over macrocycles is that a spherical cone can be modified at the cone without breaking the symmetry of the sphere whereas a macrocycle will lose its cyclic symmetry upon modification. ^{19}FIT comprises three building blocks, **I**, **II** and **III**, with **I** being the ^{19}F signal emitter and **II** and **III** being aqueous-solubility enhancers (Figure 1). ^{19}FIT was synthesized in a sequential manner that involves repetitive deprotection/condensation cycles (Scheme 1), analogous to solid-phase peptide synthesis. The synthesis proceeded from the F-sphere to the H-sphere so that all synthesis intermediates (**2**, **I**, **3**, **4**, **5**, **6** and **7**) contain nine -CF_3 groups and thereby can be purified using the unique separation power of fluorous chemistry.[18,19] The final product ^{19}FIT was purified using a combination of fluorous silica-gel chromatography and preparative HPLC (Figure S1).

^{19}FIT is soluble in phosphate buffered saline (PBS, Figure S2) and emits a single ^{19}F signal from 27 fluorine atoms (Figure 2a). ^{19}F NMR study shows that ^{19}FIT forms micelle in PBS with a critical micelle concentration *ca*. 7 mM (Figure S3). Phantom experiments show that the ^{19}F signal intensity is indeed proportional to ^{19}F concentration (Figures 2b and 2c). The ^{19}F longitudinal relaxation time, T_1, of ^{19}FIT is much shorter than that of PF15C5 measured under the same condition (163 ms vs. 1069 ms). Even with 30 mol% of relaxation enhancing Gd^{3+}, the ^{19}F T_1 of PF15C5 reported in the literature[11] is still significantly longer than that of ^{19}FIT. Shorter T_1 brings another advantage of ^{19}FIT over PFCs as it reduces data collection time and thereby increases signal intensity.[20,21]

150 mM ^{19}FIT PBS solution was administered to 16-week old BALB/c male mice at two dose levels: either 400 μL/mouse (*ca*. 60 mmol/kg ^{19}F), or 200 μL/mouse (*ca*. 30 mmol/kg ^{19}F). At both dose levels, the ^{19}F signal decreased rapidly and became invisible in all organs except the bladder after 1–2 h (Figure 3 and Figure S4). The ^{19}F signal intensity also decreased rapidly

in whole-body ^{19}F spectra and in urine samples collected from mice injected with ^{19}FIT (Figure 4a and Figure S5). Based on whole-body and urine ^{19}F signal intensity decays, the *in vivo* residence half-life, $t_{½}$, of ^{19}FIT is estimated to be *ca*. 0.5 day. In comparison, the *in vivo* residence half-lives of perfluorocarbons, also determined by ^{19}F MRI, are months or longer. [8]

Whole-body ^{19}F spectra in different mice showed only one ^{19}F peak at all time points (Figure 4b and Figure S6). There is also only one ^{19}F peak in all urine samples, with the same chemical shift as ^{19}FIT (Figure S7). Comparison of HPLC profiles of urine samples collected before and after the injection of ^{19}FIT showed only one peak contributable to fluorinated compounds (Figures 4c and 4d). The mass of this peak is 1,894.2 Da, the same as intact ^{19}FIT. All these results are consistent with no *in vivo* degradation of ^{19}FIT. Mice injected with ^{19}FIT were observed for up to 45 days and showed no sign of acute toxicity or weight loss.

In summary, ^{19}FIT overcomes major deficiencies of PFC-based ^{19}F imaging agents, including heterogeneity, instability, split ^{19}F signals, long ^{19}F T_1, complex formulation, and, most importantly, excessive organ retention. With suitable imaging agents, ^{19}F MRI has the potential to play an important role in drug therapy, analogous to the role played by ^{1}H MRI in disease diagnosis. From a chemistry standpoint, bi-spherical symmetry is a step forward from the unispherical symmetry employed in conventional dendrimer design.[22] In fact, modular symmetry is a general molecular design principle that can be extended to tri-spherical symmetry and beyond.

The application of ^{19}FIT to drug or cell monitoring via ^{19}F MRI still faces stiff challenges. One issue is sensitivity. The approach of using symmetry to generate a single ^{19}F signal from multiple fluorine atoms can only go so far, on the order of 100 fluorine atoms. Other approaches, such as using paramagnetic ions to reduce the T_1 and T_2 of ^{19}F,[11,20,21] are needed. Another issue is a dilemma common to all labeling tags. If the labeling is non-covalent, then the tag might dissociate from drugs or cells and signals from free and bound tags can hardly be distinguished. However, if the labeling is covalent, then the tag might alter the bioactivity of drugs or cells. One possible solution to this dilemma is to use the prodrug approach, i.e., making ^{19}FIT-drug into a prodrug that replaces the free drug as the therapeutic agent. The pharmacologically inactive ^{19}FIT-drug will be converted into the active free drug at the pathological site (e.g., tumor). The pharmacokinetics of ^{19}FIT-drug can be monitored with ^{19}F MRI right up to the point where ^{19}FIT-drug is converted into the free drug at the disease site, with the ^{19}FIT-drug $\rightarrow$^{19}FIT + drug conversion process monitored by ^{19}F MRS. We are currently pursing these approaches.

Experimental Section

CHEMICAL SYNTHESIS

The synthesis of ^{19}FIT involves the following steps:

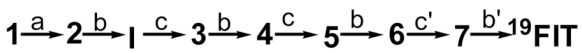

where a is ether formation, b are b′ are deprotections, c and c′ are condensations.

***tert*-butyl mono-ester 2 (procedure a)—**A suspension of potassium hydride (30%, 3.2 g, 24.0 mmol) was added slowly to a stirred solution of alcohol **1**[23] (15.8 g, 20.0 mmol) in tetrahydrofuran (200 mL) at 0 °C. After 10 min, *tert*-butyl bromoacetate (5.9 mL, 7.8 g, 40.0 mmol) was added to the suspension in one portion at rt and the resulting mixture was stirred at rt overnight. After quenching the reaction with water (20 mL), the mixture was transferred into a separatory funnel and the lower phase was collected as a clear oil. Removal of low boiling point impurities from the oil under vacuum gave the mono-ester **2** as a clear oil (14.1 g, 78%

yield). ^{1}H NMR (400 MHz, $CDCl_3$) δ 4.14 (s, 6H), 3.91 (s, 2H), 3.57 (s, 2H), 1.46 (s, 9H); ^{19}F NMR (376 MHz, $CDCl_3$) δ −73.51 (s); ^{13}C NMR (100.7 MHz, $CDCl_3$) δ 168.5, 120.2 (q, *J* = 293.4 Hz), 81.8, 79.1–80.0 (m), 69.2, 67.2, 66.2, 46.1, 27.9; MS (ESI) *m/z* 905 ((M +1)$^+$); HRMS (MALDI-TOF) calcd for $C_{23}H_{20}F_{27}O_6$ 905.0829, found 905.0823.

Mono-acid I (procedure b)—To a stirred solution of *tert*-butyl ester **2** (13.6 g, 15.0 mmol) and anisol (3.0 mL) in dichloromethane (100 mL) at rt was added trifluoroacetic acid (30 mL) and the resulting solution was stirred at rt for 2 h. After evaporated to dryness under vacuum, the residue was dissolved in methanol/toluene (50 mL/30 mL) and evaporated to dryness under vacuum to give the mono-acid **I** as a reddish oil (12.6 g, 99% yield) which was used in the next step without further purification. ^{1}H NMR (400 MHz, Acetone-*d6*) δ 4.29 (s, 6H), 4.14 (s, 2H), 3.73 (s, 2H); ^{19}F NMR (376 MHz, Acetone-*d6*) δ − 71.24 (s); ^{13}C NMR (100.7 MHz, acetone-*d*6) δ 170.9, 121.2 (q, *J* = 292.5 Hz), 80.1–81.0 (m), 68.6, 67.5, 67.1, 47.1; MS (ESI) *m/z* 848 (M$^+$); HRMS (MALDI-TOF) calcd for $C_{19}H_{12}F_{27}O_6$ 849.0203, found 849.0197.

Mono-amide 3 (procedure c)—1,3-diisopropylcarbodiimide (6.6 mL, 5.4 g, 42.5 mmol) was added to a stirred solution of 1-hydroxytriazole (5.7 g, 42.5 mmol) and acid **I** (12.0 g, 14.2 mmol) in dry *N*, *N*-dimethylformamide (200 mL) at rt. After stirring for 15 min, di-*tert*butyl iminodiacetate (**II**-(*t*Bu)$_2$) (10.4 g, 42.5 mmol) was added and the resulting mixture was stirred at rt for 12 h. Water (20 mL) was added to the reaction mixture and the resulting mixture was concentrated and purified by solid-phase extraction on Flouroflash® silica-gel, with H_2O and CH_3OH as eleunts, to give the mono-amide **3** as a clear oil (14.1 g, 92% yield) which was used in the next step without further purification. ^{1}H NMR (400 MHz, $CDCl_3$) δ 4.12 (s, 6H), 4.10 (s, 2H), 4.02 (s, 2H), 3.92 (s, 2H), 3.59 (s, 2H), 1.44 (s, 9H), 1.42 (s, 9H); ^{19}F NMR (376 MHz, $CDCl_3$) δ −73.29 (s); ^{13}C NMR (100.7 MHz, $CDCl_3$) δ 168.7, 167.9, 167.7, 120.1 (q, *J* = 293.4 Hz), 82.8, 82.0, 78.7–79.8 (m), 69.5, 67.7, 66.5, 49.9, 48.6, 46.0, 27.8, 27.76; MS (MALDI-TOF) *m/z* 1098 ((M+Na)$^+$); HRMS (MALDI-TOF) calcd for $C_{31}H_{32}F_{27}NNaO_9$ 1098.1544, found 1098.1538.

Di-acid 4 (procedure b)—This compound was prepared by employing the general procedure b. (reagents and solvent amounts were doubled compared to that of mono-acid **I**) with a 99% yield as a pale solid. ^{1}H NMR (400 MHz, CD_3OD) δ 4.22 (s, 8H), 4.16 (s, 2H), 4.14 (s, 2H), 3.60 (s, 2H); ^{19}F NMR (376 MHz, CD_3OD) δ −71.18 (s); ^{13}C NMR (100.7 MHz, CD_3OD) δ 172.5, 172.1, 171.7, 121.6 (q, *J* = 293.4 Hz), 80.4–81.5 (m), 70.3, 68.6, 67.9, 50.0, 47.4; MS (MALDI-TOF) *m/z* 964 ((M+1)$^+$); HRMS (MALDI-TOF) calcd for $C_{23}H_{17}F_{27}NO_9$ 964.0472, found 964.0476.

Tri-amide 5 (procedure c)—This compound was prepared by employing the general procedure c (reagents and solvent amount were doubled compared to that of mono-amide **3**) with a 93% yield as an oil. ^{1}H NMR (400 MHz, $CDCl_3$) δ 3.80–4.13 (m, 20H), 3.47 (s, 2H), 1.28–1.31 (m, 36H); ^{19}F NMR (376 MHz, $CDCl_3$) δ −72.94 (s); ^{13}C NMR (100.7 MHz, $CDCl_3$) δ 169.2, 169.1, 168.2, 167.6, 167.5, 167.45, 167.3, 120.0 (q, *J* = 293.4 Hz), 82.9, 82.6, 81.8, 81.5, 78.7–79.8 (m), 68.3, 67.4, 66.6, 50.4, 50.1, 49.3, 48.9, 47.6, 46.6, 45.8, 27.5, 27.4; MS (MALDI-TOF) *m/z* 1456 ((M+K)$^+$); HRMS (MALDI-TOF) calcd for $C_{47}H_{58}F_{27}KN_3O_{15}$ 1456.3074, found 1456.3327.

Tetra-acid 6 (procedure b)—This compound was prepared by using the general procedure b (reagents and solvent amount were quadrupled compared to that of mono-acid **I**) with a 99% yield as a pale wax. ^{1}H NMR (400 MHz, CD_3OD) δ 4.15 (s, 2H), 4.05–4.09 (m, 10H), 3.90–4.01 (m, 6H), 3.53–3.59 (m, 2H), 3.43 (s, 2H); ^{19}F NMR (376 MHz, CD_3OD) δ −71.13 (s); ^{13}C NMR (100.7 MHz, CD_3OD) δ 172.5, 172.4, 172.3, 172.15, 172.0, 171.6, 171.0, 121.6 (q, *J* = 292.6 Hz), 80.4–81.5 (m), 69.7, 69.1, 68.7, 68.2, 67.5, 50.5, 50.3, 49.8, 49.77, 47.3; MS

(MALDI-TOF) *m/z* 1216 ($(M+Na)^+$); HRMS (MALDI-TOF) calcd for $C_{31}H_{26}F_{27}N_3NaO_{15}$ 1216.0830, found 1216.0820.

Hepta-amide 7 (procedure c ′)—1,3-Diisopropylcarbodiimide (6.6 mL, 5.3 g, 42.0 mmol) was added to a stirred solution of 1-hydroxybenzotriazole (5.7 g, 42.0 mmol), 4 Å molecular sieve (5.0 g) and tetra-acid **6** (6.3 g, 5.3 mmol) in dry *N*, *N*-dimethylformamide (150 mL) at rt. After stirring for 15 min, 1-phenyl-2, 5, 8, 11-tetraoxatridecan-13-amine (**III**-Bn)[24] (10.0 g, 35.2 mmol) was added and the resulted mixture was stirred for 18h at rt. The mixture was filtrated, concentrated and purified by solid-phase extraction on Flouroflash® silica gel to give crude product. Then, a second coupling procedure as above mentioned was repeated with the crude product. After purification by solid-phase extraction on Flouroflash® silica-gel with H_2O and CH_3OH as eleunts, hepta-amide **7** was prepared as a clear oil (10.7 g, 90% yield). ^1H NMR (400 MHz, $CDCl_3$) δ 7.25–7.36 (m, 20H), 4.55 (s, 8H), 4.07–4.16 (m, 14H), 3.90–3.95 (m, 6H), 3.50–3.68 (m, 58H), 3.37–3.43 (m, 10H); ^{19}F NMR (376 MHz, $CDCl_3$) δ −73.47 (s); ^{13}C NMR (100.7 MHz, $CDCl_3$) δ 169.8, 169.7, 169.1, 168.9, 168.7, 168.3, 168.0, 138.0, 128.3, 127.7, 127.4, 120.0 (q, *J* = 293.3 Hz), 79.3–79.9 (m), 73.1, 70.8, 70.3, 70.0, 69.9, 69.8, 69.3, 69.1, 69.0, 68.3, 67.4, 66.4, 52.8, 52.7, 52.6, 48.3, 47.2, 45.8, 39.3, 39.2; MS (MALDI-TOF) *m/z* 2277 ($(M+Na)^+$); HRMS (MALDI-TOF) calcd for $C_{91}H_{118}F_{27}N_7NaO_{27}$ 2277.7576, found 2277.7494.

^{19}FIT (procedure b′)—A mixture of hepta-amide **7** (5.5 g, 2.5 mmol) and palladium on carbon (10%, 2.5 g) in methanol (200 mL) was stirred under an atmosphere of 50 bar hydrogen over 12 h at rt. After filtering the mixture through a pad of celite, the mixture was concentrated and purified by HPLC on preparative Fluoroflash® column with H_2O and CH_3OH as eleunts to give the pure **^{19}FIT** as a wax (4.5 g, 97% yield). The purity of ^{19}FIT was verified using analytical HPLC (Figure S1). ^1H NMR (400 MHz, CD_3OD) δ 4.26 (s, 2H), 4.25 (s, 8H), 4.22 (s, 2H), 4.18 (s, 2H), 4.15 (s, 2H), 4.05 (s, 2H), 4.04 (s, 2H), 3.59–3.67 (m, 42H), 3.53–3.58 (m, 16H), 3.44 (t, *J* = 4.2 Hz, 4H), 3.38 (t, *J* = 5.6 Hz, 4H); ^{19}F NMR (376 MHz, CD_3OD) δ −71.05 (s); ^{13}C NMR (100.7 MHz, CD_3OD) δ 172.3, 171.9, 171.3, 171.27, 171.1, 170.8, 170.5, 121.6 (q, *J* = 292.5 Hz), 80.3–81.5 (m), 73.7, 71.6, 71.4, 71.2, 71.18, 71.1, 70.4, 70.3, 69.5, 68.7, 68.3, 62.2, 53.2, 53.0, 52.5, 49.7, 47.2, 40.5, 40.4; MS (MALDI-TOF) *m/z* 1916 ($(M+Na)^+$); HRMS (MALDI-TOF) calcd for $C_{63}H_{94}F_{27}N_7NaO_{27}$ 1916.5664, found 1916.5642.

MRI and Metabolic studies—See Supporting Information.

Supplementary Material

Refer to Web version on PubMed Central for supplementary material.

References

1. Lauterbur PC. Angew. Chem 2005;117:1026–1034.Angew. Chem. Int. Ed 2005;44:1004–1011.
2. Mansfeld P. Angew. Chem 2004;116:5572–5580.Angew. Chem. Int. Ed 2004;43:5456–5464.
3. Yu J-X, Kodibagkar VD, Cui W, Mason RP. Curr. Med. Chem 2005;12:819–848. [PubMed: 15853714]
4. Wolf W, Presant CA, Waluch V. Adv. Drug. Del. Rev 2000;41:55–74.
5. Holland GN, Bottomley PA, Hinshaw WS. J. Magn. Reson 1977;28:133–136.
6. Lauterbur PC. Nature 1973;242:190–191.
7. Mason RP, Antich PP, Babcock EE, Gerberich JL, Nunnally RL. Magn. Reson. Imag 1989;7:475–485.
8. Meyer KL, Carvlin MJ, Mukherji B, Sloviter HA, Joseph PM. Invest. Radiol 1992;27:620–627. [PubMed: 1428740]
9. Morawski AM, Winter PM, Yu X, Fuhrhop RW, Scott MJ, Hockett F, Robertson JD, Gaffney PJ, Lanza GM, Wickline SA. Magn. Reson. Med 2004;52:1255–1262. [PubMed: 15562481]

10. Ahrens ET, Flores R, Xu H, Morel PA. Nat. Biotech 2005;23:983–987.
11. Neubauer AM, Myerson J, Caruthers SD, Hocket FD, Winter PM, Chen J, Gaffney PJ, Robertson JD, Lanza GM, Wickline SA. Magn. Reson. Med 2008;60:1066–1072. [PubMed: 18956457]
12. Janjic JM, Srinivas M, Kadayakkara DKK, Ahrens ET. J. Am. Chem. Soc 2008;130:2832–2841. [PubMed: 18266363]
13. Kimura A, Narazaki M, Kanazawa Y, Fujiwara H. Magn. Reson. Imag 2004;22:855–860.
14. Nosé Y. Artificial Organs 2004;28:807–812. [PubMed: 15320944]
15. Gore J. New. Eng. J. Med 2003;349:2290–2292. [PubMed: 14668454]
16. Willmann JK, van Bruggen N, Dinkelborg LM, Gambhir SS. Nat. Rev. Drug Disc 2008;7:591–607.
17. Strickley RG. Pharm. Res 2004;21:201–230. [PubMed: 15032302]
18. Horváth IT, Rábai J. Science 1994;266:72–75. [PubMed: 17814001]
19. Curran DP. Synlett 2001;9:1488–1496.
20. Ratner AV, Quay S, Muller HH, Simpson BB, Hurd R, Young SW. Invest. Radiol 1989;24:224–227. [PubMed: 2753638]
21. Lee H, Price RR, Holburn GE, Partain CL, Adams MD, Catheris WP. J. Magn. Reson. Imag 1994;4:609–613.
22. Tomalia DA, Reyna LA, Svenson S. Biochem. Soc. Trans 2007;35:61–67. [PubMed: 17233602]
23. Jiang Z-X, Yu YB. Tetrahedron 2007;63:3982–3988. [PubMed: 18461118]
24. Jiang Z-X, Yu YB. Synthesis 2008:215–220.

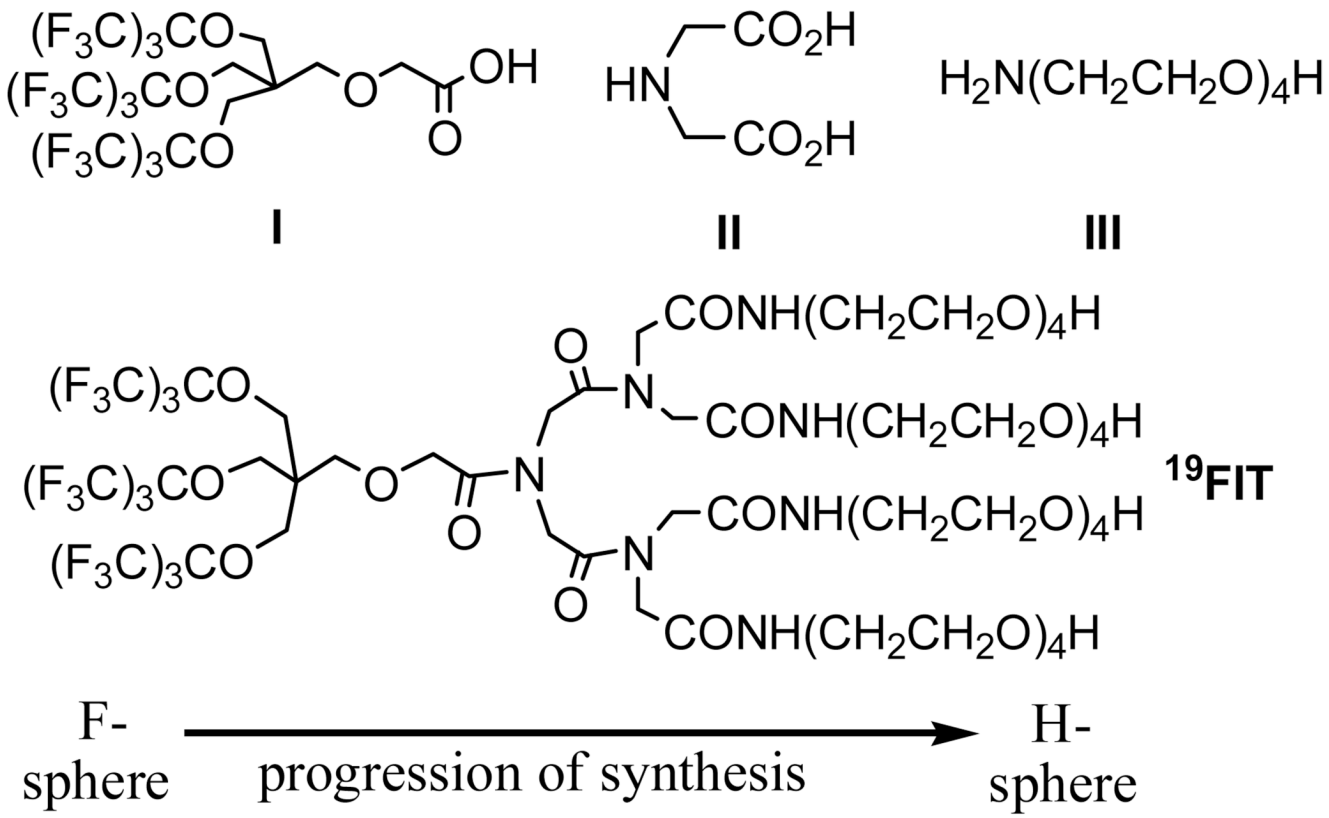

Figure 1.
Chemical structures of ^{19}FIT and its three building blocks (**I**, **II** and **III**). ^{19}FIT is designed to be a bi-spherical cone. The F-sphere contains 27 fluorine atoms for ^{19}F signal generation. The H-sphere, currently made of 4 -OH groups, can be derivatized to –COOH, -NH_2 and –SH for future drug conjugation.[23]

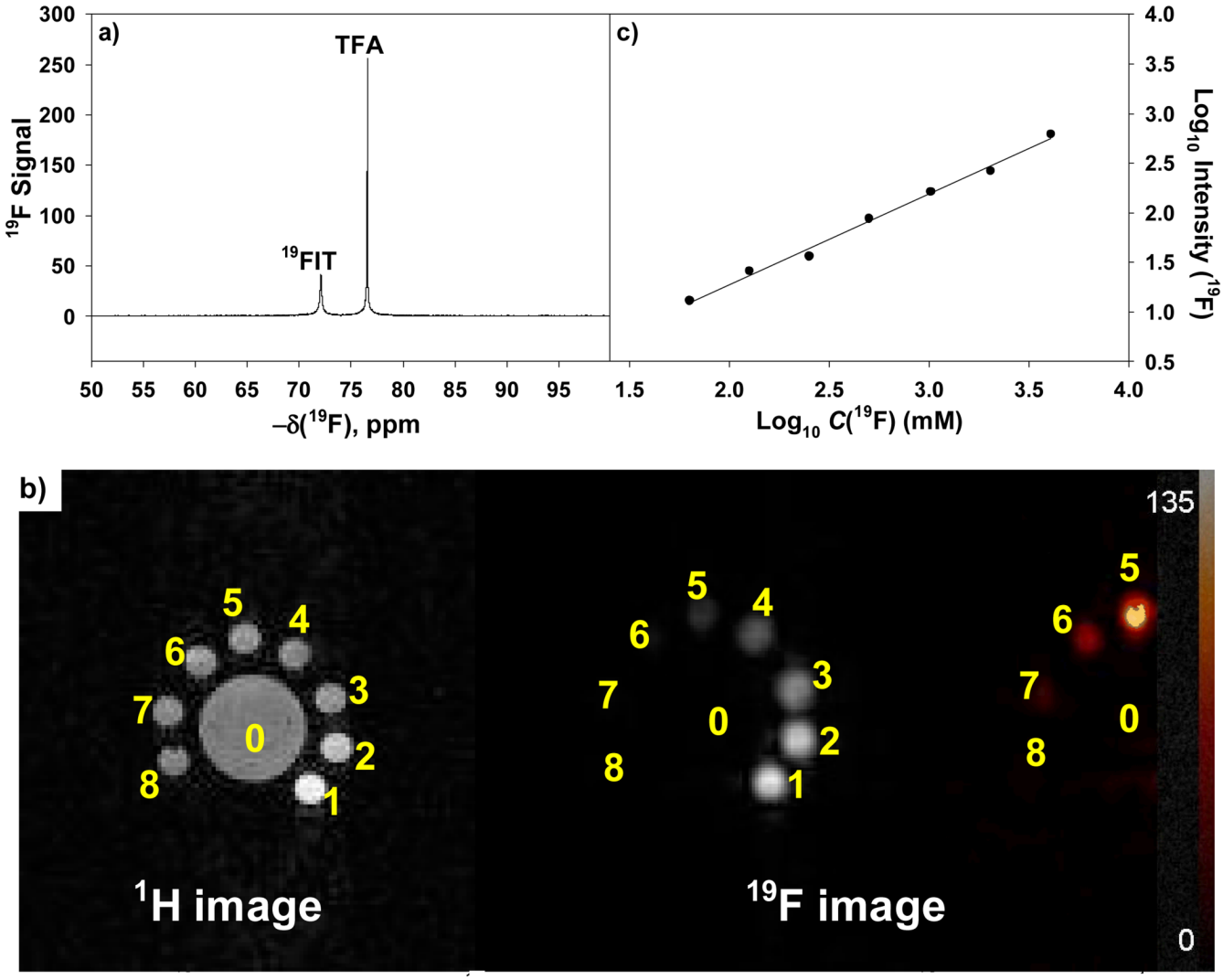

Figure 2.

a) ^{19}F NMR spectrum of ^{19}FIT in PBS. TFA is the internal ^{19}F standard. **b**) ^{1}H and ^{19}F MRI images of phantoms (1–8) filled with ^{19}FIT in PBS. ^{19}F concentrations in the phantoms are: 4,050 mM, 2,025 mM, 1,012 mM, 506 mM, 253 mM, 126 mM, 63 mM, 32 mM for phantoms 1–8, respectively. Phantom 0 contains water. ^{19}F images of the phantoms were given in two color schemes: white/black (for high concentration phantoms) and red/black (for low concentration phantoms). **c**) ^{19}F signal intensity *vs*. ^{19}F concentration.

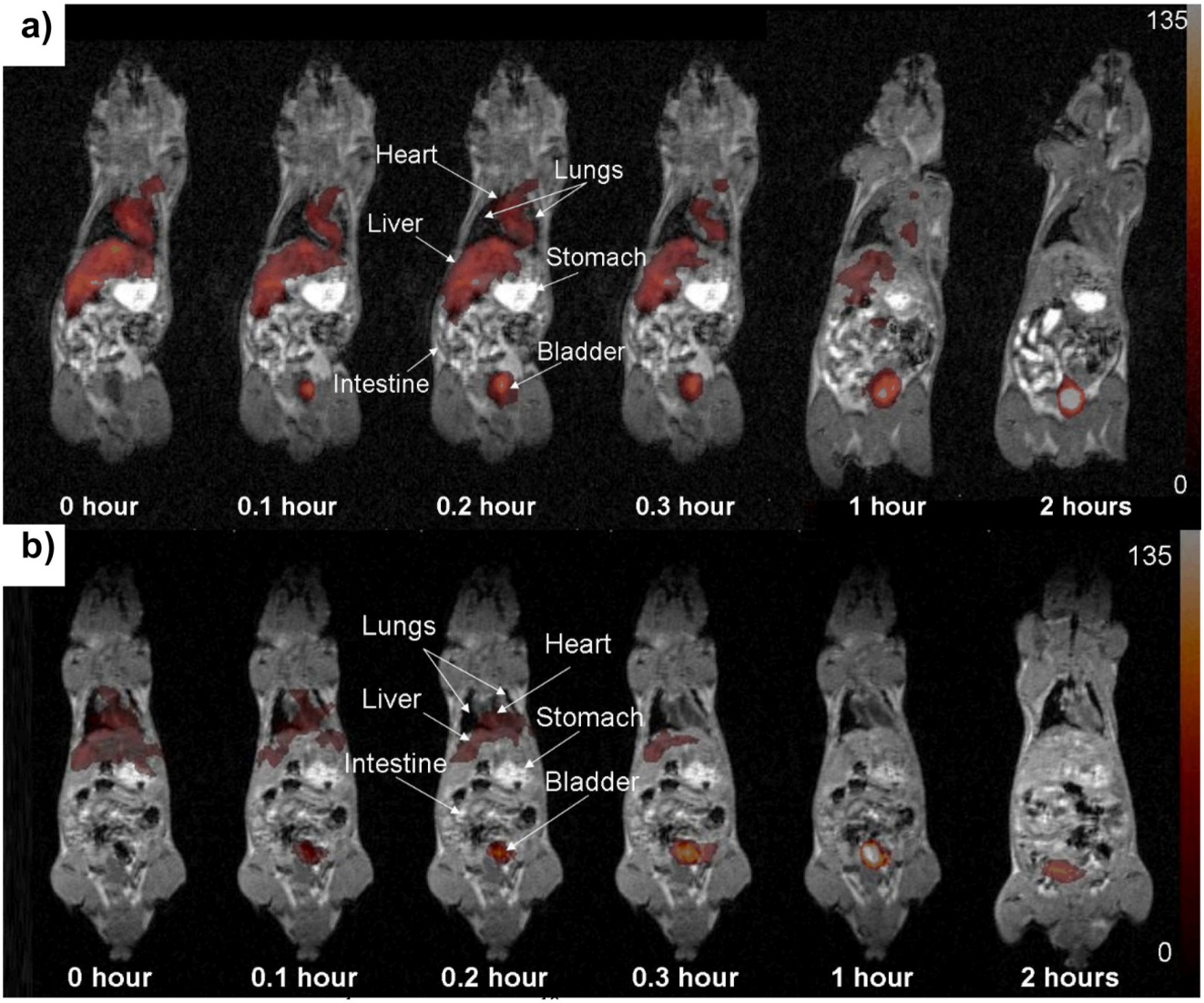

Figure 3.

Superimposed ^{1}H (white) and ^{19}F (red) images (coronal view) of mice 1 (**a**) and 3 (**b**). Mice 1 and 3 were injected with 400 μL (60 mmol/kg ^{19}F) and 200 uL (30 mmol/kg ^{19}F) of 150 mM ^{19}FIT PBS solution, respectively. For images beyond 2 h, see Figure S4.

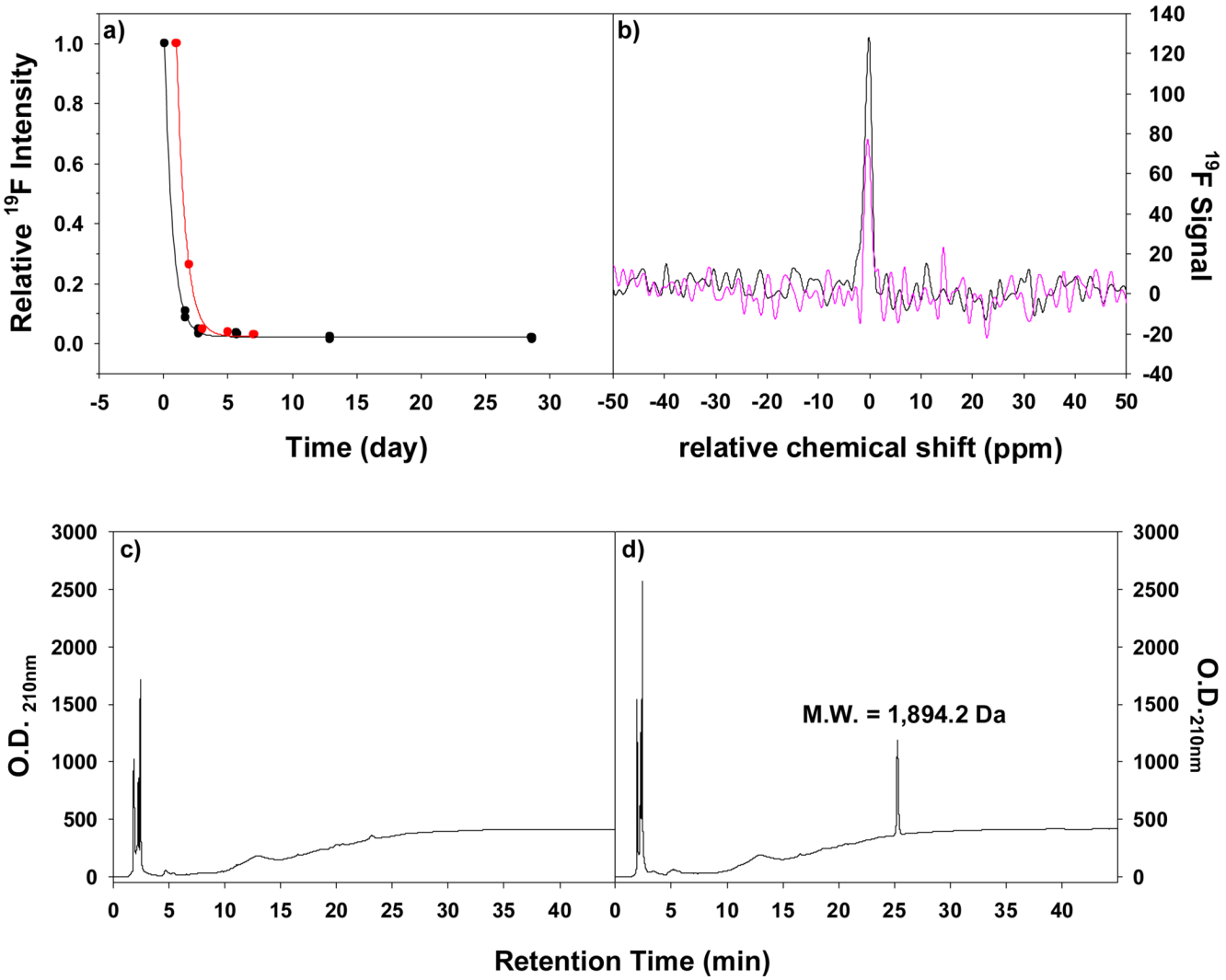

Figure 4.

a) ^{19}F signal intensity decay with time. Black symbols: whole-body ^{19}F signals from mice 1 and 2 collected using a 3.0 T clinical MR scanner. Red symbols: mouse 6 urine ^{19}F signal collected using an 11.7 T NMR spectrometer. For each series, the first data point is normalized to 1. The curves are fitting data to single component exponential decay. **b)** *In vivo* ^{19}F spectra for mouse 1 at 8220 min (black) and mouse 3 at 8880 min (pink). The maximum position of each signal is manually set to 0 ppm. The ratio of the two signal intensity is 2.08, about the same as the dose ratio between these two mice, which is 2.0. For more *in vivo* ^{19}F spectra, see Figure S6. **c, d**) HPLC chromatograms of urine collected from mouse 6 one day before (**c**) and one day after (**d**) receiving ^{19}FIT.

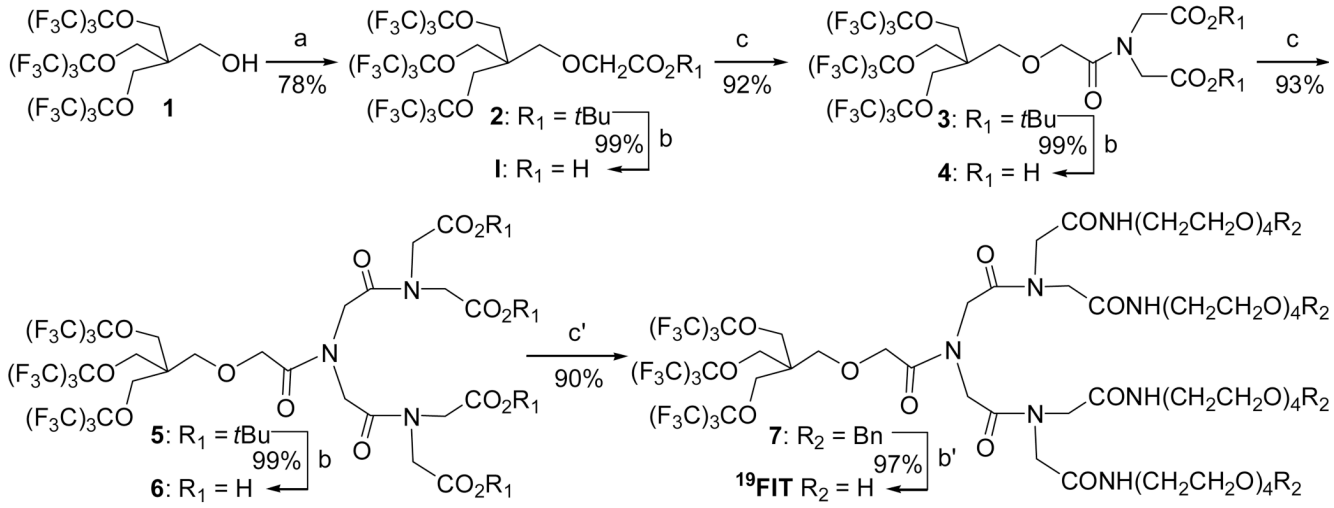

Scheme 1.

Synthesis of ^{19}FIT. Reaction Conditions: (a) KH, $BrCH_2CO_2tBu$, THF, rt, 12 h; (b) TFA, anisol, CH_2Cl_2, rt, 2 h; (c) DIC, HOBt, DMF/THF (1/1), $HN(CH_2CO_2tBu)_2$ (= **II**-(tBu)$_2$), rt, 12 h; (c′) DIC, HOBt, DMF/THF (1/1), $H_2N(CH_2CH_2O)_4Bn$ (= **III**-Bn), rt, 18 h; (b′) H_2, Pd/C, MeOH, rt, 12 h. b and b’ are deprotections while c and c’ are condensations.